Harnessing Wrinkling Patterns Using Shape Memory Polymer Microparticles

Wenbing Li, Yanju Liu, and Jinsong Leng*

Read Online

ACCESS | Metrics & More | Article Recommendations

ABSTRACT: Shape memory polymers (SMPs) are the simplest and most attractive alternatives for soft substrates of typical bilayer wrinkle systems because of shape fixity and recovery capabilities. Herein, we have successfully programmed large compressive strains in chemical cross-linking shape memory polystyrene (PS) microparticles via nanoimprint lithography, which acted as the substrate of a wrinkle system using a gold nanoparticle (Au NP) film as the top layer. When triggered by two different stimuli (direct heating and toluene vapors), the thin Au NP film could transform into various wrinkle structures atop the recovered PS particles. In addition, we also investigated the evolution mechanisms of wrinkling by heating and toluene vapors and tuned the wrinkled surfaces through altering the Au NP thickness and stimulation methods (direct heating and toluene vapors), which utilized the structural adjustability of Au NPs to program the amplitude, wavelength, and morphology of the wrinkles. The concept presented here provides a cost-effective approach to realize the surface wrinkling and can be extended to other available SMPs.

KEYWORDS: *Janus particles, wrinkle patterns, shape memory, polystyrene microparticles, actuation methods*
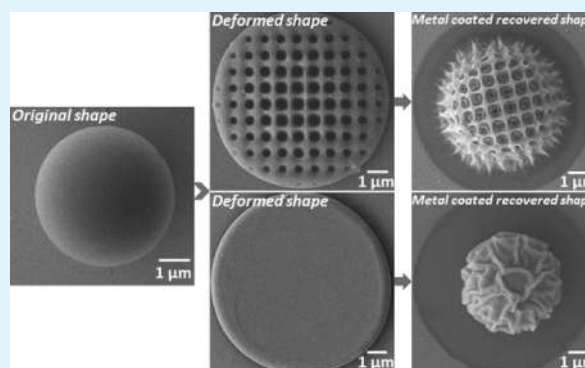
1. INTRODUCTION

Compressing a stiff thin film on a soft thick substrate can result in the spontaneous formation of regular surface wrinkling patterns.[1−8] Surface wrinkle patterns can occur in various morphologies and geometry configurations because of the differences in applied stress states. Mechanical buckling instability can easily produce wrinkling patterns and is broadly used in generating well-organized wrinkle structures on a submicrometer or micrometer scale.[9,10] A variety of applications of such wrinkled topologies have been proposed, including photonics,[11,12] smart adhesion,[13] stretchable electronics,[14] switchable wettability,[15] cellular targeting and sensing,[16,17] templates for assembling colloidal particles,[18,19] substrates for liquid manipulation and liquid crystal alignment,[20] stretchable electrodes or supercapacitors,[21,22] and a measurement method for yielding the elastic moduli of polymeric thin films.[2]

Various approaches have been used to fabricate different types of wrinkled patterns, such as thermal expansion mismatch, diffusion, oxidation, capillary force, and shape memory effect.[1,7,23−25] Most of the wrinkling studies in the literature have been conducted on the surfaces of soft polymer matrices. The wrinkle patterns generated on shape memory polymer (SMP) substrates have high structural tunability and are more flexible, convenient, rapid, and inexpensive compared to the patterns generated by other approaches. The capability

of SMPs to quickly and easily produce multiscale wrinkle structures will help scientists to further enhance the understanding between wrinkle structures and functionalities and will enable engineers to fleetly model and design particular devices based on wrinkle patterns.

In this study, we presented a simple method to fabricate wrinkle patterns through the deposition of gold nanoparticles (Au NPs) atop precompressed shape memory polystyrene (PS) microparticles. The PS microparticles were programmed via thermal embossing nanoimprint lithography (TE-NIL). Then, Au NPs were deposited on the surface of deformed microparticles by vacuum spraying. Since SMPs have the ability to fix strain without an external force,[26−29] the capability of shape recovery (shape memory effect) of SMPs can be used to form wrinkle structures.[30,31] Utilizing such a convenient and flexible approach, a series of wrinkle patterns atop shape memory PS microparticles under different stimuli (heating and toluene vapors) have been demonstrated. In addition, this study also investigated the mechanisms of wrinkling by
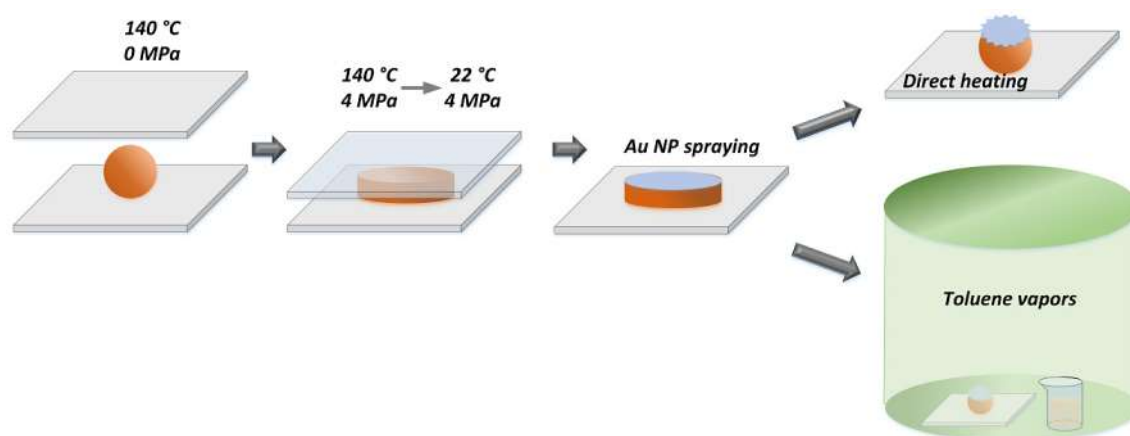
Figure 1. Schematics of the programming of PS microparticles with TE-NIL, spraying of Au NPs, and wrinkling during shape recovery by direct heating and toluene vapor stimuli.
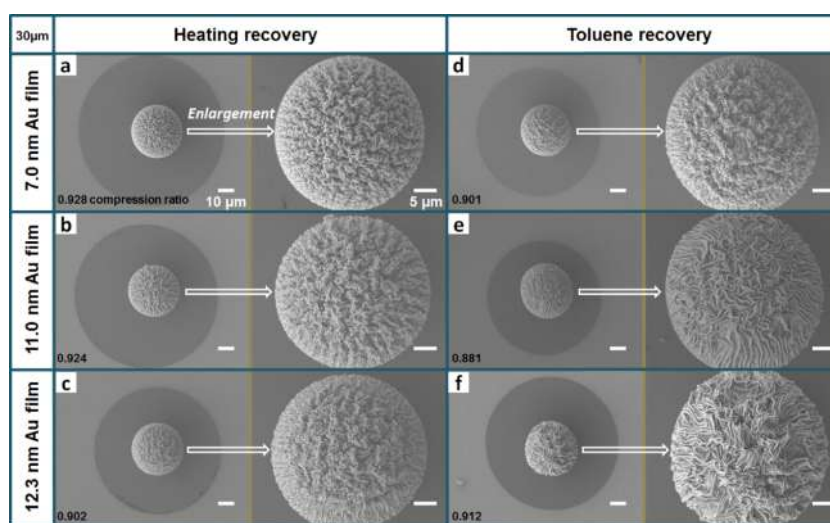
Figure 2. Wrinkled morphologies of recovered PS microparticles (30 μm) with 7.0, 11.0, and 12.3 nm Au films after heating at 140 °C for 2 h (a–c) and being immersed in toluene vapors for 6 h at room temperature (d–f).

comparing the wrinkle morphologies under two different stimulus conditions, opening up broad prospects for the development of this technology.

2. EXPERIMENTAL SECTION

2.1. Materials. PS particles with 30 and 200 μm diameter and 2% cross-linking density were purchased from Sigma-Aldrich. The 4.94 μm PS particles with 2% cross-linking density were purchased from Bangs Laboratories, Inc. The toluene and acetone were obtained from Sigma-Aldrich.

2.2. Preparation. Previous to the TE-NIL process, the silicon wafers used for depositing particles were first cleaned with acetone solution and deionized water. Second, the aqueous solution containing PS particles was dispersed using a vortex mixer for 3 min before being dropped onto the wafer surface through a dropper, and the solid-to-liquid ratio of PS particles to deionized water is 5% (w/v). Third, the wafers with PS aqueous solution were dried for 24 h at room temperature. Finally, when the deionized water evaporated completely, the dried particles dispersed on the surface of wafers were obtained for the following programming experiment.

2.3. Programming of Particles. All TE-NIL procedures were performed on a nanoimprinter (Eitre 3, Obducat), and the conditions, 140 °C, 4 MPa, 15 min, were used for the 30 and 4.94 μm PS particles. TE-NIL is an effective preparation method that is able to compress two parallel rigid sheets using different pressures.[32−34] The

deformation and shape recovery process of particles with the TE-NIL process are schematized in Figure 1. First, the PS microspheres were deposited on the surface of wafer via drip coating. Second, the particles were imprinted with a flat wafer mold under a preset pressure at 140 °C. Finally, the temperature was cooled to room temperature while the pressure remained constant. Hence, when the pressure was released, the temporary disklike shape could be fixed. After this process, the upper wafer was removed from the flattened particles that used to spray Au NPs and recover to form wrinkles by direct heating at 140 °C for 2 h and immersing in toluene vapors for 6 h at room temperature. In addition, the micropatterns (microholes or micropillars) on the PS particle surfaces are formed through the same method, except that one of the flat wafer molds is replaced by a micropatterned (micropillars or microholes) silicon wafer mold.

2.4. Characterization. For the wrinkling experiment, a metal spraying machine (SC-3000, CVC Products Inc.) was used to deposit Au films onto the flattened PS particle surface, and the thickness was tuned by controlling the spraying time. Field emission scanning electron microscopy (JSM-7401F, JEOL Ltd., Japan) was used to characterize the morphologies of PS particles and the wrinkles. The surface topographies of the samples were quantitatively analyzed with an atomic force microscope (AFM, DI 3100, Bruker, USA). The measurements were implemented at three randomly selected surface locations for each sample.
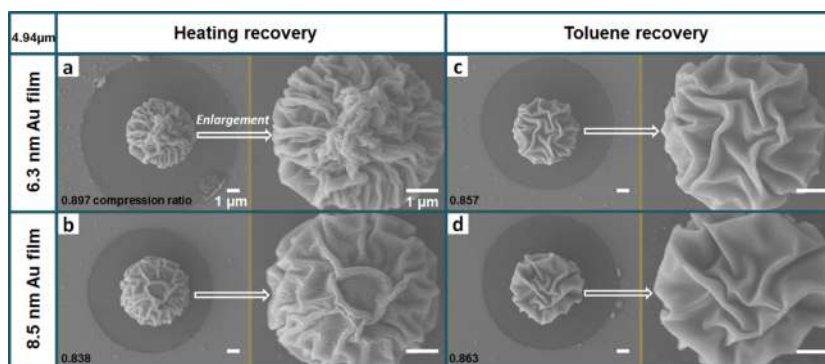
Figure 3. Wrinkled morphologies of recovered PS microparticles (4.94 μm) with a 6.3 and 8.5 nm Au layers after heating at 140 °C for 2 h (a,b) and being immersed in toluene vapors for 6 h at room temperature (c,d).
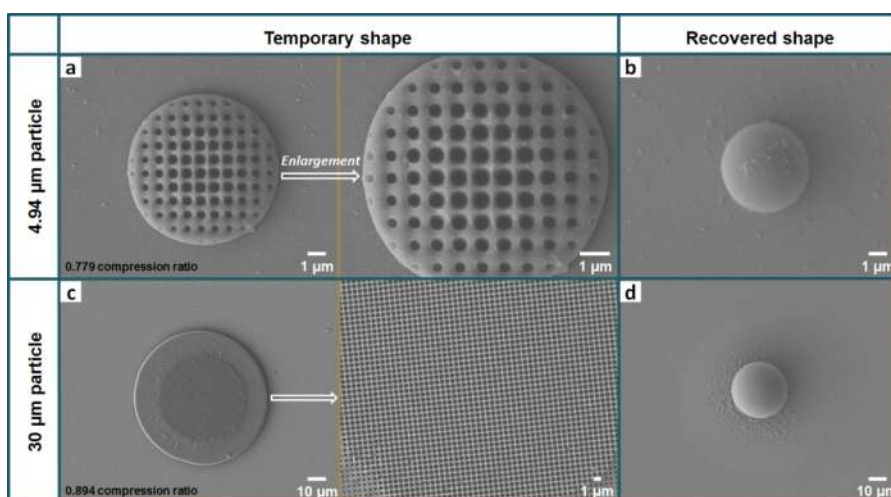
Figure 4. SEM images showing the PS particles after compression, programmed temporary micropatterns, and recovery. Microhole-patterned temporary shapes of the (a) 4.94 and (c) 30 μm PS particles. Recovered shapes of the (b) 4.94 and (d) 30 μm PS particles after heating at 140 °C for 2 h.

2.5. Image Processing. The compression ratios and the dimension of the characteristic wrinkles were quantified to research their relationship with the morphology features. These were measured after image postprocessing by ImageJ software. In detail, the original SEM images of the PS particles were opened using ImageJ. Based on the distance in pixels of the known scale length, we could measure the areas and sizes of the flattened particles and the wrinkles formed by shape recovery.

3. RESULTS AND DISCUSSION

3.1. Characterization of Surface Wrinkling. To generate wrinkled Au NP layers, we introduced a method for the spraying of Au NPs onto the surface of deformed shape memory PS particles. This process included impressing the PS particles by the TE-NIL procedure, spraying a certain thickness layer of Au NPs, and actuating temporary shape recoveries via direct heating and toluene vapor stimuli (Figure 2). The deformed PS particles (30 μm) were heated above their glass transition temperature (T_g of PS ≈100 °C) at 140 °C for 2 h (Figure 2a−c) and placed into a homemade closed device saturated with toluene vapors for 6 h (Figure 2d−f) at room temperature. Because of the mismatch in Poisson's ratios of the stiffer Au NP film and the soft polymer substrate, the recovery of flattened particles upon heating induced a mechanical compression on the Au NP layer. Then, the mechanical compression in the Au NP film will be alleviated through the

buckling of the film layer and leads to a wrinkled surface.[25,35] When exposed to the vapors, in fact, increasing the fraction of toluene solvent in PS particles generates a similar result to heating. Adding solvent to a glassy polymer can indeed reduce its T_g, to a temperature even lower than the environmental temperature.[36] Hence, the flattened particles shrunk and also induced surface wrinkling. From Figure 2, in the case of the two different stimuli, we can see that there are two kinds of wrinkle patterns, labyrinthine wrinkles in the central areas and azimuthal wrinkles along the particle edges. The amplitude and area of the azimuthal wrinkles increase with an increase in the Au NP layer thickness. From Figure 2c,f, the protrusion forms in the center of the labyrinthine wrinkle patterns. The hierarchical wrinkling patterns are generated because of the latitudinal compressive stress during the shape recovery of the deformed particle. Nevertheless, the anisotropic latitudinal strain is larger than the isotropic strain in the region far away from the central protrusion. Hence, anisotropic radial wrinkles are formed in this region.[30] Amazingly, we observed that the wrinkle patterns of heat-induced recovery and toluene-induced recovery with the same Au NP film layer thickness were obviously different. Compared with the heat-induced recovery, in the toluene-induced recovery process, the surface topography becomes more hierarchical, showing a combination of small ridges and larger features. From Figure 2e,f, the ridgelike skin layer morphologies with high aspect ratios were observed,
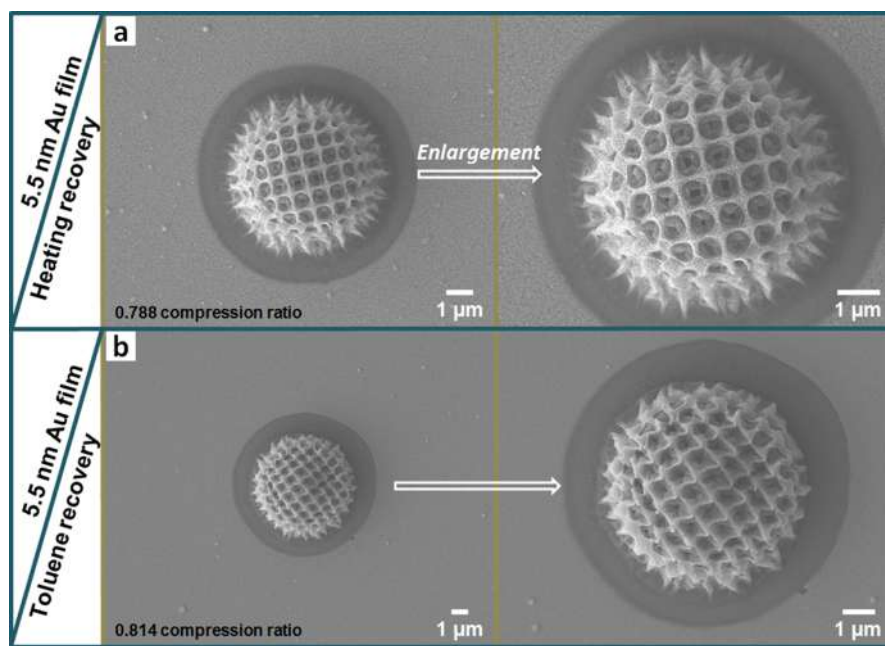
Figure 5. Wrinkled morphologies of microhole-patterned 4.94 μm PS particles with a 5.5 nm Au film after heating at 140 °C for 2 h (a) and being immersed in toluene vapors for 6 h at room temperature (b).
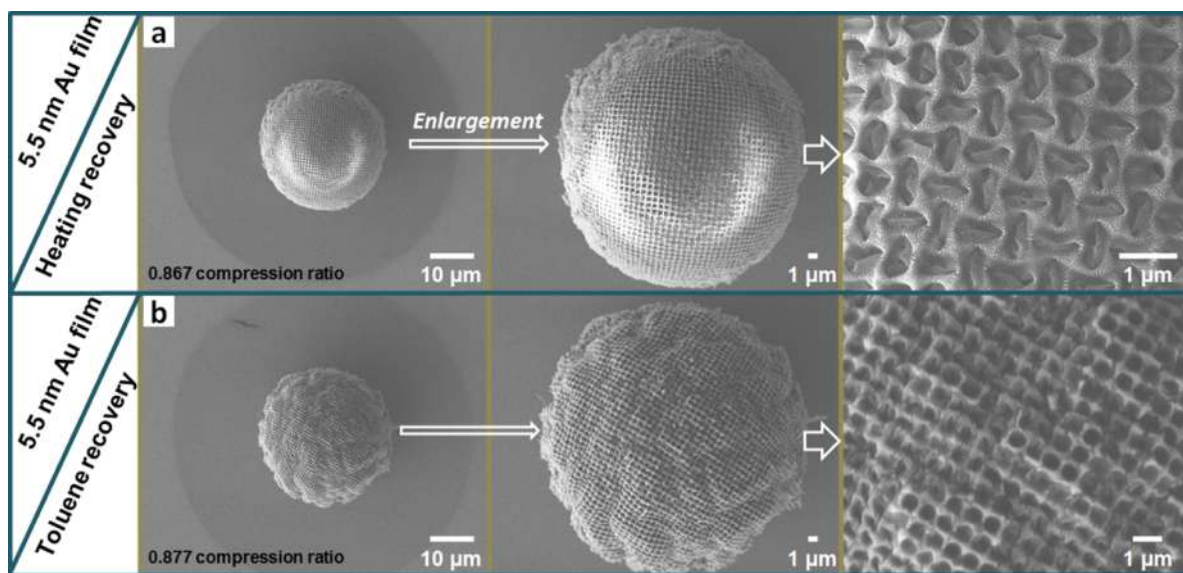
Figure 6. Wrinkled morphologies of microhole-patterned 30 μm PS particles with a 5.5 nm Au film after heating at 140 °C for 2 h (a) and being immersed in toluene vapors for 6 h at room temperature (b).

of which both the feature size and the degree of hierarchy increase with an increase in the Au NP thickness.[37]

Compared with 30 μm particles, we have also studied the phenomenon of surface wrinkling with 4.94 μm PS particles. As shown in Figure 3, the 4.94 μm particles exhibited a similar wrinkling characteristic, and the stripe-shaped wrinkles of toluene-induced recovery (Figure 3c,d) are also larger than those of the heat-induced recovery (Figure 3a,b). There may be two possible reasons. First, during immersion in toluene vapors, the inner osmotic pressure induced by the prior swelling of the PS particles led to a net compressive stress in the system.[7,38] Once the stress surpassed the critical threshold value,[39] the pattern morphology of surface wrinkles started to form and significantly depended on the thickness of the Au NP

layer. Second, when the toluene fraction exceeded a critical value, the T_g of the PS reduced to a temperature below the ambient temperature, then the temporary flattened PS particles began to recover, and the coated Au film subsequently contracted in the latitudinal direction with the PS substrate. Similarly, it suffered a latitudinal compressive stress in that direction. During shape recovery, the Au film layer buckles on the basis of previous wrinkles induced by the toluene solvent swelling; hence, there is a larger fold (wavelength and amplitude) because of the synergistic effect of previous swelling and later shape recovery. In addition, the area of central protrusion became larger with an increase in the compression ratio of the particle using direct heating (Figure 3a). The reason is that the amplitudes of the first-generation
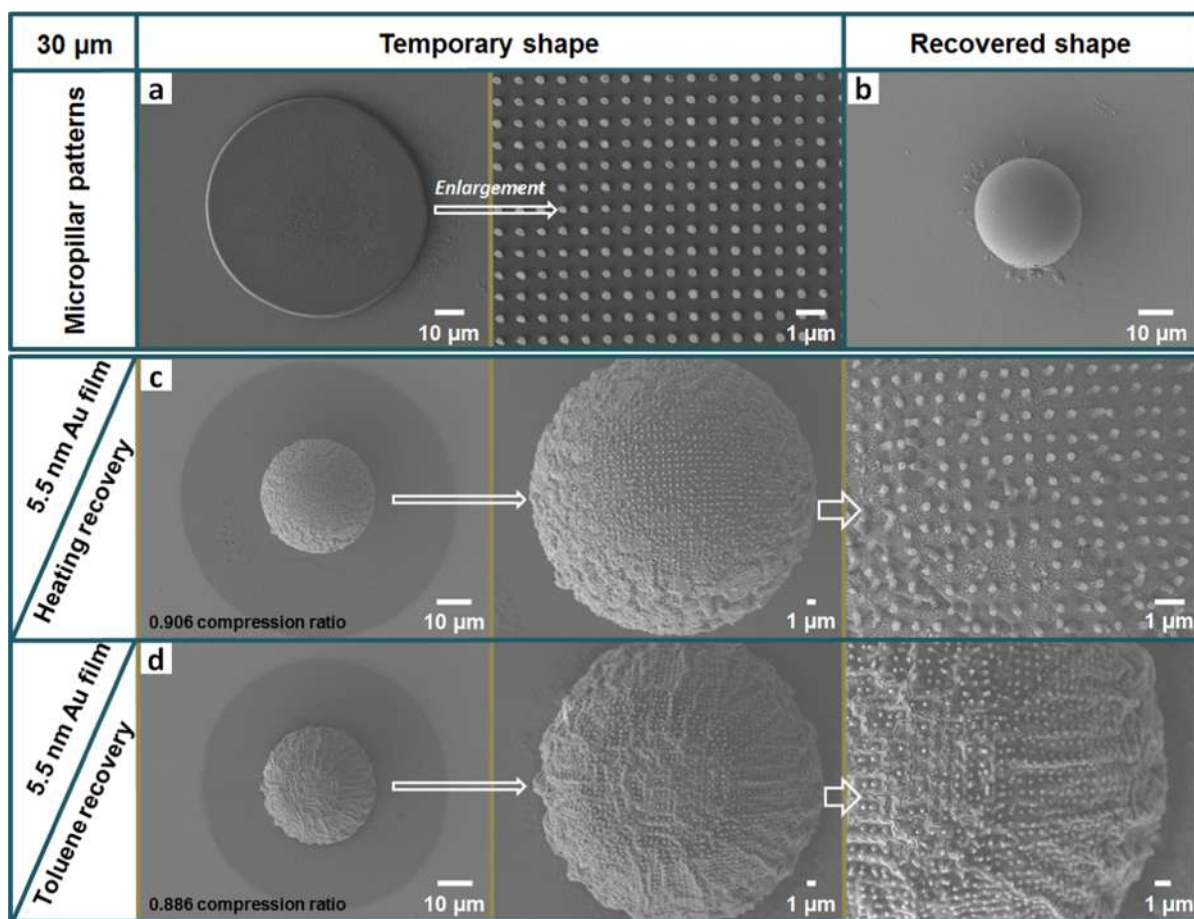
Figure 7. SEM images showing the PS particles after compression, programmed temporary micropatterns, and recovery. (a) Micropillar-patterned temporary shape of the 30 μm PS particle. (b) Recovered shape of the 30 μm PS particle when triggered by toluene stimulus for 6 h. Wrinkled morphology of the micropillar-patterned 30 μm PS particles with a 5.5 nm Au film after (c) heating at 140 °C for 2 h and (d) immersing in toluene vapors for 6 h at room temperature.

wrinkles saturate and further form a new and hierarchical stiffer protrusion when the compressive stress becomes large (0.897 compression ratio).[3,33]

To better utilize the unique features of the PS particles, we also investigated how the wrinkles formed on the patterned PS particle surfaces. As shown in Figure 4a,c, the deposited particles (4.94 and 30 μm) were successfully programmed to hold microhole-patterned temporary shapes with high compression ratios. When these deformed particles (shown in Figure 4b,d) were heated at 140 °C for 2 h, they could recover to their original shapes significantly.

To investigate the specificity of the wrinkled morphology generated on the microhole-patterned particle surfaces during the shape recovery, the programmed PS particles (4.94 μm) were sprayed with a 5.5 nm thick Au NP coating. Figure 5a shows the recovered particle after heating, and Figure 5b shows the recovered particle that was stimulated by toluene vapors. From Figure 5, the particles subjected to two different stimuli exhibited partial recoveries of their initial shapes (including the particle matrix and patterned surface). The reason may be that the Au NP film coating restricts the shape recovery of the matrix and patterned surface of the PS microparticles. It is worth mentioning that, with heat- and toluene-induced recovery processes, different Janus particles can be obtained. The shape of heat-induced recovery resembled that of a sunflower, and the shape of toluene vapor-induced recovery

resembled that of a metal net. In the future, we believe that these unique morphologies, fabricated for the first time in this study, can be used for target applications in different fields.

For comparison, we have also investigated the wrinkled morphology generated on the microhole-patterned 30 μm PS particle surfaces coated by the Au NP layer with the same thickness (5.5 nm). Similar to 4.94 μm PS particles, we obtain different recovered morphologies through heating (Figure 6a) and toluene vapor (Figure 6b) stimuli. However, in contrast to 4.94 μm particles, the circular patterns are deformed severely, as shown in Figure 6a,b (see the enlarged image), and the Au NP layer of toluene-induced recovery is partially cracked (view the enlarged image of Figure 6b). We believe that it is related to the compression ratios of the PS particles. The origin of surface cracking is most probably because of the latitudinal deformation caused by Poisson's effect, which leads to the fracture of the Au NP layer when the latitudinal deformation reaches its failure strain.[39] Because the compression ratio of 30 μm PS particles is larger than that of 4.94 μm particles, the deformed particles (30 μm) recovered by toluene vapors have the maximum compression ratio of 0.877 (Figure 6b).

Taking 30 μm PS particles as an example, compared with the micropore patterns, we have also studied the effect of micropillar patterns on wrinkling using heating and toluene stimuli. Figure 7a shows the micropillar-patterned temporary shape, and Figure 7b shows the recovered shape after toluene
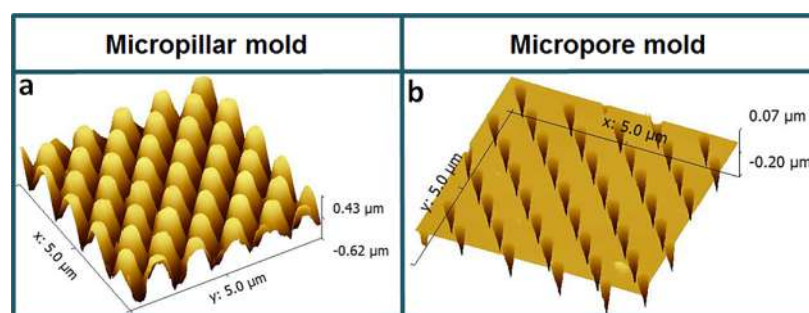
Figure 8. Topographic AFM images of programmed micropillar (a) and micropore (b) molds. All AFM images are 5 μm × 5 μm in size.

stimulus for 6 h. Just like in the oven (shown in Figure 4), the toluene stimulus can also well induce the shape recovery of the prepatterned PS microparticles. As shown in Figure 7c,d, these SEM images show the recovered morphologies of the micropillar-patterned surface induced by heating and toluene vapors after gold spraying, respectively. However, it is noteworthy that the wrinkling caused by the two stimuli (heating and toluene vapors) is not obvious. The possible reason is that part of the deposited thin Au NP film bends convexly because of the shape recovery of the PS particles upon heating. Herein, however, the film stress is compressed by the recovery stress of micropillars; thus, no wrinkle is formed. But at the same time, the Au NP layer also constrains the shape recovery of the micropillars. While in the toluene-induced recovery process (Figure 7d), because there is a synergistic effect of particle swelling and shape recovery after being immersed in the toluene vapors, slight radial-shaped wrinkles appeared.

The micrometer-scaled patterns (micropillars and micro-pores) on the silicon wafer molds are fabricated by the photolithography method, followed by the inductive coupled plasma etching process. After that, PS particles, which are predeposited on the surfaces of unpatterned silicon wafers, are imprinted under the patterned silicon molds. The micro-patterns are formed temporarily onto the surfaces of the particles by the TE-NIL method. By peeling the PS particles off from the micropillar-patterned and micropore-patterned silicon molds, the SMP micropores and micropillars are obtained, respectively. Herein, the topologies and sizes of the two molds, which were used for controlling the deformation of the particles, are shown in the AFM images (Figure 8). The orthogonally arrayed square micropillars have a peak-to-peak distance of 0.8 μm, diameter of the pattern base of 0.8 μm, and diameter at the pattern peak of 0.3 μm, and the peak-to-valley height of the pattern is about 0.8–0.9 μm (Figure 8a). The distance from the center of the micropore to the center is 0.8 μm, the diameter of the micropore at the surface is 0.3 μm, and the maximum depth at the deepest point is 0.2 μm, as shown in Figure 8b.

4. CONCLUSIONS

In conclusion, we presented a novel method to fabricate tunable wrinkles induced by a compressive stress on Au NP films atop shape memory PS microparticles, because of the expansion mismatch and shape memory effect. Furthermore, the evolution of the wrinkle pattern via heating and toluene vapor stimuli is systemically investigated to reveal the impact of the shape memory effect and expansion mismatch. In addition, we could control the size, arrangement, and

morphology of Au NP wrinkles by varying the driving method, programming temporary micropatterns on the surface of the deformed PS particles, and tuning the thickness of the Au NP layer. Thus, compared to static particles, such smart PS particles and wrinkled metal films could have exciting potential applications in sensors, catalysis, drug delivery, magnetic biomarkers, and optoelectronics.

■ AUTHOR INFORMATION

Corresponding Author
Jinsong Leng − *Centre for Composite Materials and Structures, Harbin Institute of Technology (HIT), Harbin 150080, PR China;* ⊙ orcid.org/0000-0001-5098-9871; Email: lengjs@hit.edu.cn

Authors
Wenbing Li − *Centre for Composite Materials and Structures, Harbin Institute of Technology (HIT), Harbin 150080, PR China; Key Laboratory of Eco-Textiles, Ministry of Education, Jiangnan University, Wuxi 214122, PR China;* ⊙ orcid.org/0000-0002-6867-8884

Yanju Liu − *Department of Astronautical Science and Mechanics, Harbin Institute of Technology (HIT), Harbin 150001, PR China*

Complete contact information is available at:
https://pubs.acs.org/10.1021/acsami.1c00623

Notes
The authors declare no competing financial interest.

■ REFERENCES

(1) Bowden, N.; Brittain, S.; Evans, A. G.; Hutchinson, J. W.; Whitesides, G. M. Spontaneous Formation of Ordered Structures in Thin Films of Metals Supported on an Elastomeric Polymer. *Nature* **1998**, *393*, 146−149.

(2) Stafford, C. M.; Harrison, C.; Beers, K. L.; Karim, A.; Amis, E. J.; VanLandingham, M. R.; Kim, H. C.; Volksen, W.; Miller, R. D.;

Simonyi, E. E. A Buckling-Based Metrology for Measuring the Elastic Moduli of Polymeric Thin Films. *Nat. Mater.* **2004**, *3*, 545−550.

(3) Efimenko, K.; Rackaitis, M.; Manias, E.; Vaziri, A.; Mahadevan, L.; Genzer, J. Nested Self-Similar Wrinkling Patterns in Skins. *Nat. Mater.* **2005**, *4*, 293−297.

(4) Efimenko, K.; Finlay, J.; Callow, M. E.; Callow, J. A.; Genzer, J. Development and Testing of Hierarchically Wrinkled Coatings for Marine Antifouling. *ACS Appl. Mater. Interfaces* **2009**, *1*, 1031−1040.

(5) Khang, D. Y.; Rogers, J. A.; Lee, H. H. Mechanical Buckling: Mechanics, Metrology, and Stretchable Electronics. *Adv. Funct. Mater.* **2009**, *19*, 1526−1536.

(6) Yang, S.; Khare, K.; Lin, P. C. Harnessing Surface Wrinkle Patterns in Soft Matter. *Adv. Funct. Mater.* **2010**, *20*, 2550−2564.

(7) Chung, J. Y.; Nolte, A. J.; Stafford, C. M. Diffusion-Controlled, Self-Organized Growth of Symmetric Wrinkling Patterns. *Adv. Mater.* **2009**, *21*, 1358−1362.

(8) Chung, J. Y.; Nolte, A. J.; Stafford, C. M. Surface Wrinkling: A Versatile Platform for Measuring Thin-Film Properties. *Adv. Mater.* **2011**, *23*, 349−368.

(9) Singamaneni, S.; Tsukruk, V. V. Buckling Instabilities in Periodic Composite Polymeric Materials. *Soft Matter* **2010**, *6*, 5681−5692.

(10) Watanabe, M.; Mizukami, K. Well-Ordered Wrinkling Patterns on Chemically Oxidized Poly(dimethylsiloxane) Surfaces. *Macromolecules* **2012**, *45*, 7128−7134.

(11) Kolaric, B.; Vandeparre, H.; Desprez, S.; Vallee, R. A. L.; Damman, P. In Situ Tuning the Optical Properties of a Cavity by Wrinkling. *Appl. Phys. Lett.* **2010**, *96*, No. 043119.

(12) Koo, W. H.; Jeong, S. M.; Araoka, F.; Ishikawa, K.; Nishimura, S.; Toyooka, T.; Takezoe, H. Light Extraction from Organic Light-Emitting Diodes Enhanced by Spontaneously Formed Buckles. *Nat. Photonics* **2010**, *4*, 222−226.

(13) Chan, E. P.; Smith, E. J.; Hayward, R. C.; Crosby, A. J. Surface Wrinkles for Smart Adhesion. *Adv. Mater.* **2008**, *20*, 711−716.

(14) Khang, D. Y.; Jiang, H.; Huang, Y.; Rogers, J. A. A Stretchable Form of Single-Crystal Silicon for High-Performance Electronics on Rubber Substrates. *Science* **2006**, *311*, 208−212.

(15) Lin, P. C.; Yang, S. Mechanically Switchable Wetting on Wrinkled Elastomers with Dual-Scale Roughness. *Soft Matter* **2009**, *5*, 1011−1018.

(16) Wu, L. Y.; Ross, B. M.; Hong, S.; Lee, L. P. Bioinspired Nanocorals with Decoupled Cellular Targeting and Sensing Functionality. *Small* **2010**, *6*, 503−507.

(17) Xiang, T.; Hou, J.; Xie, H.; Liu, X.; Gong, T.; Zhou, S. Biomimetic Micro/Nano Structures for Biomedical Applications. *Nano Today* **2020**, *35*, No. 100980.

(18) Horn, A.; Hiltl, S.; Fery, A.; Boker, A. Ordering and Printing Virus Arrays: A Straightforward Way to Functionalize Surfaces. *Small* **2010**, *6*, 2122−2125.

(19) Pazos-Pérez, N.; Ni, W.; Schweikart, A.; Alvarez-Puebla, R. A.; Fery, A.; Liz-Marzán, L. M. Highly Uniform SERS Substrates Formed by Wrinkle-Confined Drying of Gold Colloids. *Chem. Sci.* **2010**, *1*, 174−178.

(20) Ohzono, T.; Monobe, H. Microwrinkles: Shape-Tunability and Applications. *J. Colloid Interface Sci.* **2012**, *368*, 1−8.

(21) Pegan, J. D.; Ho, A. Y.; Bachman, M.; Khine, M. Flexible Shrink-Induced High Surface Area Electrodes for Electrochemiluminescent Sensing. *Lab Chip* **2013**, *13*, 4205−4209.

(22) Chen, T.; Xue, Y. H.; Roy, A. K.; Dai, L. M. Transparent and Stretchable High-Performance Supercapacitors Based on Wrinkled Graphene Electrodes. *ACS Nano* **2014**, *8*, 1039−1046.

(23) Qi, L.; Ruck, C.; Spychalski, G.; King, B.; Wu, B.; Zhao, Y. Writing Wrinkles on Poly(dimethylsiloxane) (PDMS) by Surface Oxidation with a CO_2 Laser Engraver. *ACS Appl. Mater. Interfaces* **2018**, *10*, 4295−4304.

(24) Huang, J.; Juszkiewicz, M.; De Jeu, W. H.; Cerda, E.; Emrick, T.; Menon, N.; Russell, T. P. Capillary Wrinkling of Floating Thin Polymer Films. *Science* **2007**, *317*, 650−653.

(25) Gabardo, C. M.; Yang, J.; Smith, N. J.; Adams-mcgavin, R. C.; Soleymani, L. Programmable Wrinkling of Self-Assembled Nano-particle Films on Shape Memory Polymers. *ACS Nano* **2016**, *10*, 8829−8836.

(26) Xie, T. Tunable Polymer Multi-Shape Memory Effect. *Nature* **2010**, *464*, 267−270.

(27) Li, W. B.; Liu, Y. J.; Leng, J. S. Selectively Actuated Multi-Shape Memory Effect of a Polymer Multicomposite. *J. Mater. Chem. A* **2015**, *3*, 24532−24539.

(28) Li, W.; Liu, Y.; Leng, J. Programmable and Shape-Memorizing Information Carriers. *ACS Appl. Mater. Interfaces* **2017**, *9*, 44792−44798.

(29) Lendlein, A.; Langer, R. Biodegradable, Elastic Shape-Memory Polymers for Potential Biomedical Applications. *Science* **2002**, *296*, 1673−1676.

(30) Zhao, Y.; Huang, W. M.; Fu, Y. Q. Formation of Micro/Nano-Scale Wrinkling Patterns Atop Shape Memory Polymers. *J. Micromech. Microeng.* **2011**, *21*, No. 067007.

(31) Zhao, Y.; Huang, W. M.; Wang, C. C. Thermo/Chemo-Responsive Shape Memory Effect for Micro/Nano Surface Patterning Atop Polymers. *Nanosci. Nanotechnol. Lett.* **2012**, *4*, 862−878.

(32) Wang, Z.; Hansen, C.; Ge, Q.; Maruf, S. H.; Ahn, D. U.; Qi, H. J.; Ding, Y. Programmable, Pattern-Memorizing Polymer Surface. *Adv. Mater.* **2011**, *23*, 3669−3673.

(33) Cox, L. M.; Killgore, J. P.; Li, Z.; Zhang, Z.; Hurley, D. C.; Xiao, J.; Ding, Y. Morphing Metal-Polymer Janus Particles. *Adv. Mater.* **2014**, *26*, 899−904.

(34) Cox, L. M.; Sun, X.; Wang, C.; Sowan, N.; Killgore, J. P.; Long, R.; Wu, H. A.; Bowman, C. N.; Ding, Y. Light-Stimulated Permanent Shape Reconfiguration in Cross-Linked Polymer Microparticles. *ACS Appl. Mater. Interfaces* **2017**, *9*, 14422−14428.

(35) Li, J.; An, Y.; Huang, R.; Jiang, H.; Xie, T. Unique Aspects of a Shape Memory Polymer as the Substrate for Surface Wrinkling. *ACS Appl. Mater. Interfaces* **2012**, *4*, 598−603.

(36) Vandeparre, H.; Gabriele, S.; Brau, F.; Gay, C.; Parker, K. K.; Damman, P. Hierarchical Wrinkling Patterns. *Soft Matter* **2010**, *6*, 5751−5756.

(37) Wang, M.; Gorham, J. M.; Killgore, J. P.; Omidvar, M.; Lin, H.; DelRio, F. W.; Cox, L. M.; Zhang, Z.; Ding, Y. Formation of a Crack-Free, Hybrid Skin Layer with Tunable Surface Topography and Improved Gas Permeation Selectivity on Elastomers Using Gel-Liquid Infiltration Polymerization. *ACS Appl. Mater. Interfaces* **2017**, *9*, 28100−28106.

(38) Chan, E. P.; Crosby, A. J. Spontaneous Formation of Stable Aligned Wrinkling Patterns. *Soft Matter* **2006**, *2*, 324−328.

(39) Chung, J. Y.; Youngblood, J. P.; Stafford, C. M. Anisotropic Wetting on Tunable Micro-Wrinkled Surfaces. *Soft Matter* **2007**, *3*, 1163−1169.